

P. W. Doll*, M. Wolf, M. Weichert, R. Ahrens, B. Spindler, and A. E. Guber

Nanostructuring of Titanium by Anodic Oxidation with Sulfuric and Hydrofluoric Acid

Abstract: Within this work we demonstrate different Anodic Oxidation processes to achieve a broad variety of nanostructures on titanium and the titanium alloy Ti6Al4V for the use as medical implant surfaces. The influence of electrolyte, reaction time and voltage on the nanostructure formation is described as well as the transfer to microstructured surfaces. As electrolytes we investigate sulfuric and hydrofluoric acids with different concentrations. The resulting nanostructures reach from nano porosities over amorphous sponge like structures to self-assembled hexagonal nanotubes.

Keywords: Titanium, Ti6Al4V, Nanotubes, Anodic Oxidation

<https://doi.org/10.1515/cdbme-2018-0154>

1 Introduction

Commercially pure Titanium Grade 4 and the Titanium alloy Ti6Al4V are widely used in medical applications such as pace makers, endoprosthesis or dental implants [1]. The success of an implantation of such devices is often limited due to biofilm formation on the surface of the medical implant [2]. Once a biofilm has formed, implant associated infections are the result and more often the implant has to be removed. To prevent biofilm formation nanostructures can be applied to the implant surface [3, 4]. Many different mechanisms to create such structures are available in literature [3-5]. One elegant way to create self-assembled homogeneous nanostructures in form of so called nanotubes

is the method of Anodic Oxidation [6, 7]. With this process it is possible to create a broad variety of different nanostructures reaching from nano porosities over amorphous sponge like structures to regular hexagonal arranged nanotubes.

2 Materials and Methods

2.1 Substrate Material

Since pure Titanium (cpTi) and the Titanium alloy Ti6Al4V (Ti6Al4V) are often used as implant materials we investigated the formation of nanostructures on these two materials. The material was provided by Cendres+Métaux SA (Biel, Switzerland) as 1 m long bars with diameters of 8 mm.

2.2 Substrate Preparation

The bars were cut into 200 mm rods and a 2 mm wide flat was milled into the bars. This flat acts as a reference within different measurement equipment like Atomic Force Microscopy (AFM) or Scanning Electron Microscopy (SEM). The bars were cut into 2 mm disks by wire cutting and grinded and polished to a defined surface finish. For one batch of fabrication 91 samples were placed on a flange and then grinded with silicon carbide paper with different grid sizes (P400, P800, P1200 to P2500, Struers GmbH). Between each step the complete flange was intensely cleaned with deionized water (DI-water). All samples have been uniquely marked using a Laser marking system containing the batch and sample number. After marking the samples were removed from the flange, turned over and the other side was also grinded with the same parameters than the first side. Subsequently a final polishing step was performed by mechanically/chemically polishing using a mixture of colloidal silicon particle solution (OP-S Nondry, Struers GmbH) and hydrogen peroxide (31%, BASF SE) of 9:1. The polishing procedure was performed 2 times for 10 min at

*Corresponding author: Doll P. W.: Karlsruhe Institute of Technology, Institute of Microstructure Technology, Hermann-von-Helmholtz-Platz 1, 76344 Eggenstein-Leopoldshafen, Germany, e-mail: patrick.doll@kit.edu

Wolf M., Weichert M., Ahrens R., Guber A. E.: Karlsruhe Institute of Technology, Institute of Microstructure Technology, Hermann-von-Helmholtz-Platz 1, 76344 Eggenstein-Leopoldshafen, Germany

Spindler B.: Fräszenrum Ortenau GmbH & Co.KG., Industriestr. 2-4, 77728 Ortenau; Germany

150 rpm and a force of 20 N (Saphir 355, ATM GmbH). This polishing method results in a mirror like surface finish with very small average roughness values (**Table 1**). After sample preparation the samples were removed from the flange and ultrasonically cleaned for 10 min with 2-propanol and DI-water respectively.

Table 1: Average Surface Roughness Values (R_a , R_t) and contact angle after final polishing of the cpTi and Ti6Al4V samples of one batch of sample production.

Material	R_a [nm]	R_t [nm]	Contact Angle [°]
cpTi	2.8 ± 0.3	63.4 ± 10.7	80.8 ± 0.9
Ti6Al4V	1.3 ± 0.2	27.5 ± 11.5	81.2 ± 0.6

2.3 Microstructured Surfaces

Medical implants mostly have complex 3D shapes and may be optimized by a micro structured topography e.g. in form of so called microgrooves to enhance implant/tissue interaction. To investigate the ability of the Anodic Oxidation processes, to produce the characteristic nanostructures on top of such microstructured surfaces we fabricated different test samples by UV-Lithography and wire cutting.

24 grinded and polished samples have been microstructured by UV-Lithography and wet etching as described in [9]. By controlled under etching of a structured photo resist nearly rectangular, spiked and sine-shaped microgrooves of lateral dimensions of 2.5, 5, 10 and 50 μm were fabricated. 5 additional samples have been microstructured by wire cutting by vertically cutting 100 μm into the polished surface of the sample. Applying several cuts next to each other with distances of 250 μm results in regular microgrooved surfaces with lateral sizes of 250 μm and depths of 125 μm . The slag layer was removed by wet etching with hydrofluoric acid (5%, BASF, SE) for 30 min.

2.4 Anodic Oxidation

The experimental setup consists of a reaction beaker, a power source, a special sample holder, a counter electrode made of stainless steel, an optional current sensing circuit and a PC to record the data. As electrolytes we used sulfuric acid (H_2SO_4) and hydrofluoric acid (HF), respectively. The experiments were performed at concentrations of 1, 10 and 20 wt. % H_2SO_4 and 0.5 and 1 wt. % HF. Reaction times reached from 30 s for H_2SO_4 electrolytes and up to 20 min for HF electrolytes.

2.5 Sample Characterization

For characterization the samples have been analyzed by Vertical Scanning Interferometry (VSI, ContourGT, Bruker Corp.), Scanning Electron Microscopy (Supra VP 60, Zeiss AG), Atomic Force Microscopy (DimensionsICON, Bruker Corp.) and contact angle measurements (40 Micro, Data Physics GmbH). Surface roughness values were measured by VSI with a field of view of $170 \times 130 \mu\text{m}^2$. For each sample an average of three measurements was taken. The result of one batch of production is shown in Table 1. Contact angle measurements were performed using a droplet volume of 4 μl . Three measurements per sample were taken to build an average value (Table 1).

3 Results

3.1 Influence of Electrolyte

Since Anodic Oxidation with non-fluoride containing solution differs in principle to fluoride containing electrolytes the resulting nanostructures are different in shape, size and formation [6-8]. In case of H_2SO_4 electrolyte the anodic process starts with oxide layer growth and nanostructures are built by electric breakdown and nanotube formation within this layer. As a result of re-oxidation and further electrical breakdowns a random distribution of nanotubes is formed. **Figure 1 A, B and C** show results of different Anodic Oxidation processes for 10 wt. % H_2SO_4 for 90 s at different voltages. In case of HF electrolytes the anodic process delivers hexagonally arranged nanotubes as reported by various other studies [6, 8]. **Figure 1 D, E and F** show such hexagonally arranged nanotubes which have been created using a 0.5 wt. % HF solution at different voltages of 5, 20, and 40 V and 20 min reaction time.

3.2 Influence of Voltage

For samples oxidized with H_2SO_4 electrolyte increasing voltage will firstly result in a thicker oxide layer. If the applied voltage is higher than a critical voltage depending on material, temperature and the materials surface roughness the oxide layer partly breaks down and nanostructures in form of randomly distributed nanotubes are formed. Figure 1 shows photographs of samples oxidized at different voltages and the corresponding Scanning Electron Micrographs. The nanostructure formation partly starts at 90 V as indicated by the darker spots. For 100 V and higher the whole sample

surface is evenly covered with random distributed nanotubes/pores. Since the mechanism for nanostructure formation is a different for Anodic Oxidation with HF electrolytes nanostructures are formed even at lower voltages. Figure 1 (D, E and F) shows this correlation. While the process starts with small nanoporosities with lateral sizes in the range of 20 nm the tubes are getting larger with higher voltages until at 40 V a porous sponge like structure results.

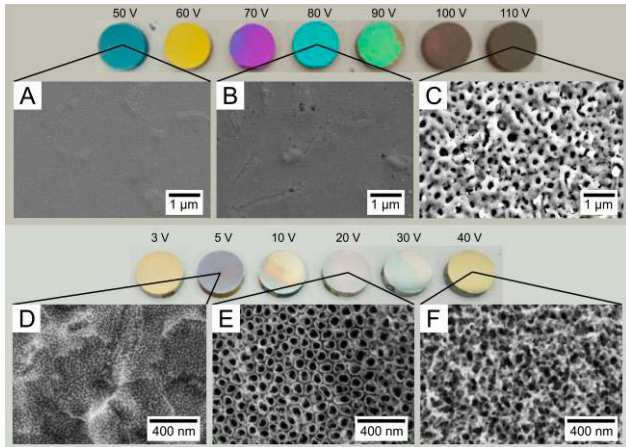


Figure 1: Photographs and corresponding Scanning Electron Micrographs of samples oxidized in 10 wt. % H_2SO_4 at different voltages (A) 30 V, (B) 80 V and (C) 110 V and in 0.5 wt. % HF at voltages of (D) 5 V, (E) 20 V and (F) 40 V.

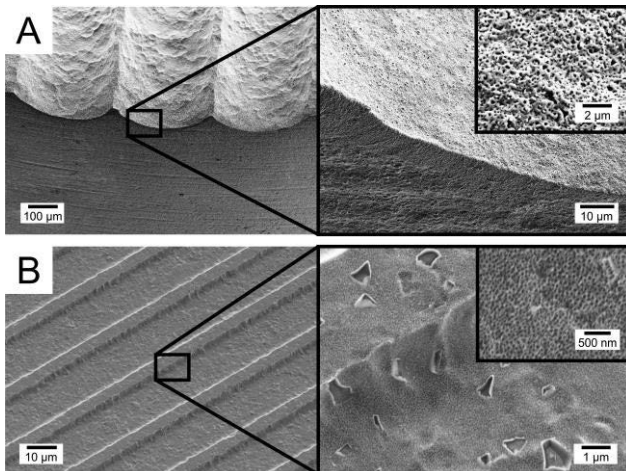


Figure 2: Scanning Electron Micrographs of hierarchically micro- and nanostructured samples which have been anodized in H_2SO_4 (A) and HF electrolyte (B).

3.3 Influence of Reaction Time

Reaction time plays an essential role in Anodic Oxidation processes. Oxide layer growth, distribution of nano pores/tubes or the arranged growth of hexagonal nanotubes take different times. For H_2SO_4 the reaction starts immediately after applying voltage with oxide layer growth and after a few seconds electric break downs within this layer occur. After 30 s some areas of the sample surface are not yet covered by nanostructures at all while for 60 s of anodization time nearly the whole surface is covered. Yet the distribution is not homogeneous. After a period of 90 s the whole sample surface is evenly covered by nanopores. In contrast to randomly distributed nanopores the growth of hexagonally arranged nanotubes by anodizing with a HF electrolyte takes much more time [8]. After 1 min the whole surface is covered with nanoporosities of around 20 nm in diameters which then grow larger with increasing reaction time (see Figure 1). After 5 min the typical hexagonally arranged nanotubes are developed. While for cpTi the nanotube layer is already evenly covering the whole sample surface the beta phase of the Ti6Al4V is still visible since it has not yet been covered by the growing oxide/nanotube layer. Further increase in time will increase the overall depth of the nanotubes and the overgrowth of the beta phase. The diameters of the nanotubes are in the range of 40 to 50 nm at this point with wall thicknesses of 10 to 15 nm referring to SEM and AFM measurements which have been carried out.

3.4 Transfer to Microtopographies

Our experiments show that Anodic Oxidation processes with HF and H_2SO_4 electrolytes can be used to apply the typical nanoporous/nanotubular structures of anodization with H_2SO_4 or HF electrolytes to micro structured topographies of a broad range of different sizes. Scanning Electron Micrographs in **Figure 2** show hierarchically nanostructured microgrooved samples which have been made by wire cutting (A) and UV-Lithography and wet etching (B) and following anodization processes. The microgrooves in Figure 2 A have lateral dimensions of 250 μm and depths of 125 μm . The microgrooves in Figure 2 B have a period of 20 μm and a depth of 4 μm . It can be seen that the whole sample surfaces are evenly covered by nanostructures resulting from Anodic Oxidation for both, H_2SO_4 and HF electrolytes. Even sharp edges can be homogeneously covered with nanostructures. The Scanning Electron Micrograph in Figure 2 B also indicates the beta phase of the Ti6Al4V material which only has been covered partly by the oxide/nanotube layer. This can be problematic for

nanostructuring of Ti6Al4V by HF anodization. Yet if reaction time or voltage is further increased the beta phase gets more and more covered. In contrast to that the coverage of beta phase for anodic oxidation in H₂SO₄ delivers similar nanotopographies for both materials.

4 Conclusion

Anodic Oxidation is an elegant method for nanostructuring titanium and Ti6Al4V material. A broad variety of different nanotopographies can be realized by variation of electrolyte, applied voltage and reaction time. In case of Anodic Oxidation with sulfuric acid (H₂SO₄) electrolytes the resulting nanostructures arrange randomly and form porous structures within the TiO₂ layer. The topography consists of evenly distributed nanopores. For hydrogen fluoride (HF) containing electrolytes the surface can be structured with various topographies reaching from nanoporosities over hexagonally arranged nanotubes to sponge like structures. We could demonstrate that both processes and the resulting nanostructures can be transferred to 3D micro topographies such as microgrooves. The resulting hierarchically micro-nanostructured surfaces can be used for 3D medical implants like dental implants or endoprosthesis.

Acknowledgment: Authors would like to thank M. Guttman, U. Köhler and H Fornasier for their help with hydrofluoric etching and anodizing. Authors would like to thank Cendres+Métaux SA for providing the titanium material.

Author Statement

Research funding: This work has been funded by the German Federal Ministry for Economic Affairs and Energy (BMWi) within the Innovation Programme ZIM for small and middle size companies (No. KF2308206KJ4). Conflict of interest: Authors state no conflict of interest. . Informed consent: Informed consent is not applicable. Ethical approval: The conducted research is not related to either human or animals use.

References

- [1] Elias C N, Lima J H C, Valiev R, Meyers M A. Biomedical Applications of Titanium and its Alloys. *JOM* 2008, 60:46.
- [2] Trampuz A, Widmer A. F. Infections associated with orthopedic implants. *Current Opinion in Infectious Diseases* 2006, 19:4.
- [3] Seddiki O, Harnagea C, Levesque L, Mantovani D, Rosei F. Evidence of antibacterial activity on titanium surfaces through nanotextures. *Applied Surface Science* 2014, 308, 275–284.
- [4] Xing R, Lyngstadaas S P, Ellingsen J E, Taxt-Lamolle S, Haugen H J. The influence of surface nanoroughness, texture and chemistry of TiZr implant abutment on oral biofilm accumulation. *Clin Oral Impl Res* 2014, 26:6.
- [5] Bhadra C M, Truong V K, Pham V T H, Al Kobaisi M, Seniutinas G, Wang J Y, Juodkazis S, Crawford R J & Ivanova E P. Antibacterial titanium nanopatterned arrays inspired by dragonfly wings. 2015, 18:5.
- [6] Dikova T D, Hahm M G, Hashim D P, Narayanan N T, Vajtai R, Ajayan P M. Mechanism of TiO₂ Nanotubes Formation on the Surface of Pure Ti and Ti-6Al-4V Alloy. *Adv Mat Res*. 2014:939: 655-662.
- [7] Ross A P, Webster T J. Anodizing color coded anodized Ti6Al4V medical devices for increasing bone cell functions. *Int J Nanomed*. 2013:8. 109-117.
- [8] Gong D, Grimes C A, Varghese O K, Hu W, Singh R S, Chen Z, Dickey E C. Titanium oxide nanotube arrays prepared by anodic oxidation. *J Mater Res* 2001. 16:12.
- [9] Doll P W, Semperowitsch C, Häfner M, Ahrens R, Spindler B, Guber A E. Fabrication of Micro Structured Dental Implant Abutments for Optimized Soft Tissue Integration. *Current Directions in Biomedical Engineering* 2018: 4(1).